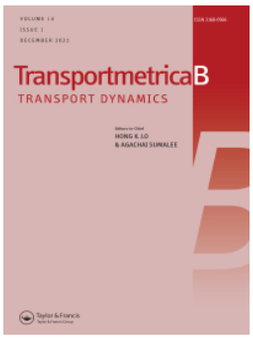

Transportmetrica B: Transport Dynamics

ISSN: (Print) (Online) Journal homepage: https://www.tandfonline.com/loi/ttrb20

Quantifying incident impacts and identifying influential features in urban traffic networks

JuYeong Lee, JiIn Kwak, YongKyung Oh & Sungil Kim

To cite this article: JuYeong Lee, JiIn Kwak, YongKyung Oh & Sungil Kim (2023) Quantifying incident impacts and identifying influential features in urban traffic networks, Transportmetrica B: Transport Dynamics, 11:1, 279-300, DOI: 10.1080/21680566.2022.2063205

To link to this article: https://doi.org/10.1080/21680566.2022.2063205

TRANSPORTMETRICA B: TRANSPORT DYNAMICS
2023, VOL. 11, NO. 1, 279–300
https://doi.org/10.1080/21680566.2022.2063205

Taylor & Francis
Taylor & Francis Group

Quantifying incident impacts and identifying influential features in urban traffic networks

JuYeong Lee [a], Jiln Kwak [b], YongKyung Oh [a] and Sungil Kim [a,b]

[a]Department of Industrial Engineering, Ulsan National Institute of Science and Technology (UNIST), Ulsan, Republic of Korea; [b]Artificial Intelligence Graduate School, Ulsan National Institute of Science and Technology (UNIST), Ulsan, Republic of Korea

ABSTRACT

Traffic incidents are a common occurrence in urban traffic networks, but predicting their impacts is challenging because of network complexity and the dynamic spatial and temporal dependencies inherent in traffic data. Nevertheless, the prediction of traffic incident impacts is crucial for global positioning systems to provide drivers with real-time route recommendations for bypassing congested roads. To this end, we formulated nonrecurrent congestion measures to quantify these impacts and developed a new method to identify the influential features that locally affect individual incidents. Because traffic incident impacts are determined by a complex entanglement of local features, a meaningful feature that can explain their impacts globally may not exist. Consequently, to identify all influential local features, we applied the local interpretable model-agnostic explanations (LIME) technique to the proposed nonrecurrent congestion measures. The proposed method was validated using real user trajectory data and incident data provided by the NAVER Corporation and the Korean National Police Agency, respectively.

ARTICLE HISTORY
Received 6 September 2021
Accepted 4 April 2022

KEYWORDS
Congestion propagation; incident impact measurement; urban traffic networks; traffic incidents

1. Introduction

Traffic congestion has become a universal problem in cities as a result of exponential population growth and the corresponding increases in number of vehicles, infrastructure, and the proliferation of delivery services. Congestion can cause various social, environmental, and economic problems such as impairing the use of transportation infrastructure and increasing travel time, air pollution, and fuel consumption.

The traffic congestion caused by a particular event, rather than by regular traffic congestion during peak hours, is called nonrecurrent traffic congestion (Hall 1993). This type of congestion occurs as a result of unexpected events such as vehicle collisions, road maintenance, or debris. Traffic incidents are the most difficult type of nonrecurrent traffic congestion to predict, but they must be handled in a timely and effective manner to minimize their impact on road capacity and travel time, and to obviate the potential for secondary crashes.

To mitigate the adverse impacts of traffic incidents, traffic agents such as transport information centers or navigation platforms must have prior knowledge regarding the characteristics of impacts and their influential features. Such knowledge enables them to provide timely and reliable information regarding route guidance in real time. Because traffic incidents occur spontaneously, a well-coordinated traffic incident management process can improve safety, traffic flow, and clearance

CONTACT Sungil Kim sungil.kim@unist.ac.kr

time (Haghani et al. 2006). Because the influence of a detected incident is typically unknown until it is completely cleared, it is essential for traffic agents to predict incident impacts beforehand.

Various attempts have been made to measure the impact of traffic incidents and construct incident impact prediction models to identify influential features. However, existing approaches are limited in various ways. First, they rely predominantly on quantitative measurements that, in practice, are not available for nonrecurrent traffic congestion. For example, the incident duration, which is one of the most popular measures related to incident impacts (Hurdle, Merlo, and Robertson 1997), requires the time interval between incident occurrence and incident site clearance to be both available and measured correctly (Ghosh, Savolainen, and Gates 2014). In the real world, such information is often unavailable, which limits the ability to define a reasonable incident duration and justify the entire process of predicting and analyzing incident impacts. Second, existing studies are primarily focused on the temporal impact of incidents without considering the spatial or speed dynamics aspects. These aspects of nonrecurrent traffic congestion require new quantitative measurements. Third, predicting nonrecurrent congestion measures is notoriously difficult because the underlying physics and interconnected congestion propagation processes are complex nonlinear turbulent dynamics problems (Chi-Sen Li and Chen 2014). The reason for this is that, in practice, perfect knowledge regarding the characteristics of an incident is never available. Consequently, errors are inevitable in the development of congestion propagation prediction models and the identification of influential features.

A global positioning system (GPS) trajectory consists of a series of points with latitude, longitude, and timestamp information generated when navigation service users travel. Based on GPS trajectory data provided by the NAVER Corporation, we previously aligned the sequence of observed user positions with the road network using a map-matching process (Newson and Krumm 2009) to obtain the average speed of each road. However, trajectory-based average road speeds are highly volatile, depending on the availability of user data over a specific period on a given road.

To overcome the limitations and difficulties outlined above, we propose new nonrecurrent congestion measures using trajectory-based average road speeds and a new method to identify the influential features that locally affect individual incidents. The main contributions of our study are summarized as follows.

- We formulated three new nonrecurrent congestion measures using trajectory-based average road speeds: incident duration, congestion propagation level, and speed drop ratio. Unlike the measures used in previous studies, these measures are applicable in the absence of accurate time information regarding an incident and can measure both the temporal and spatial impacts of incidents.
- We applied the local interpretable model-agnostic explanations (LIME) technique to the development of congestion propagation prediction models, to extract meaningful information regarding influential features related to the proposed nonrecurrent congestion measures.

The remainder of this paper is organized as follows. Section 2 reviews related work, and Section 3 defines the notations used herein. Section 4 presents our proposed novel methodology for measuring nonrecurrent traffic congestion and identifying influential features for such measures. A case study in which the proposed measures are used is presented in Section 5 and related experimental results are presented in Section 6. Finally, the conclusions of this study are summarized in Section 7.

2. Related work

2.1. Incident delay estimation

Several analytical methods have been developed to estimate the total delay of incoming roads connected to incident areas, based on classical traffic flow theory. These can be divided into two main categories, according to their approach: (1) deterministic queuing diagrams (Highway Capacity Manual 1994; Goolsby 1971; Chung and Recker 2012) and (2) shockwave theory (Wirasinghe 1978;

Chow 1976; Al-Deek, Garib, and Radwan 1995). A queuing model is constructed such that the queue lengths and wait times can be measured. The traffic shockwave theory determines the delay time by measuring the difference between the average traffic flow and density. Wirasinghe (1978) used shockwave theory to develop formulas for calculating the individual and total delays of incoming roads connected to incident areas. The formulas developed are based on the areas and densities of regions representing different traffic states. Chow (1976) compared queuing analysis and shockwave analysis for calculating the total incident delay on highways. They assumed a unique flow–density relationship and derived equations for the total delay. These methods can be used independently or combined. Wong and Wong (2016) analyzed the trajectories of GPS-equipped vehicles encountering an incident site and proposed six measures for evaluating the impact of the incident on traffic patterns based on classical traffic flow theory.

However, these approaches have limited ability to measure the impact of nonrecurrent traffic congestion propagation. First, to quantify incident impacts, they rely on various traffic features which are typically unavailable in practice, such as traffic flow, density, and occupancy. Second, they presume that the exact times of traffic incident occurrence and recovery are known, which is not always the case in reality.

2.2. Traffic congestion measures

Numerous studies have considered urban traffic conditions using various methods based on multiple measures that evaluate traffic states. The speed reduction index (SRI) ratio was proposed to measure the relative speed variation between a congested state and free-flow conditions, where congestion was defined as an index value exceeding a specific threshold (He et al. 2016; Shunping, Hongqin, and Shuang 2011). The Urban Congestion Report of 2019, published by the Federal Highway Administration, defines the free-flow speed as the 85th percentile of off-peak speed measures. This refers to the average speed from 9:00 AM to 4:00 PM and from 7:00 PM to 10:00 PM on Mondays through Fridays, and on Saturdays and Sundays from 6:00 AM to 10:00 PM. He et al. (2016) developed the speed performance index by considering the maximum permissible speed as the free-flow speed.

The methods discussed above define traffic congestion based on measurements falling below a certain threshold. However, these measures overly simplify actual incident duration periods and the duration of the incident impacts. Additionally, any incident that significantly affects neighboring roads, but does not exceed the threshold, would be ignored if the threshold speed limit determined the start and recovery times of an incident. Therefore, it is reasonable to capture nonrecurrent congestion by measuring the relative speed decline compared to the regular road speed.

2.3. Feature importance for incident impacts

Existing approaches to modeling incident impacts can be divided into two main categories: statistical methods and machine learning (ML).

The most popular statistical approaches to modeling incident duration are regression models and hazard-based models. These similarly rely on rigorous mathematical assumptions to interpret the relationships between estimators and explanatory features (Karlaftis and Vlahogianni 2011). Regression models include both linear and nonparametric regression (Garib, Radwan, and Al-Deek 1997; Peeta, Ramos, and Gedela 2000; Khattak, Schofer, and Wang 1994). Hazard-based models are superior for capturing duration effects (Chung 2010; Hojati et al. 2013; Chung and Yoon 2012) and can be categorized into three main methods: proportional hazard models (Breslow 1975), accelerated failure time models (Nam and Mannering 2000; Hojati et al. 2013), and Cox proportional hazard regression models (Bennett 1999; Lee and Fazio 2005). Another frequently used method for modeling traffic incident impact is the cell-transmission model (CTM) proposed by Daganzo (1994). Yaping Li et al. (2015) and Ji, Zhang, and Sun (2011) modified CTM to analyze and predict the impact of traffic incidents. Ji et al. (2009) used CTM to model the incident recovery time.

However, because these statistical methods operate under several hypotheses and constraints, they often lose interpretive and prediction power, leading to the necessity of nonlinear methods such as machine learning (ML).

ML approaches have been employed successfully to estimate and predict traffic incident duration and interpret models, because they can describe influential features (Ruimin Li, Pereira, and Ben-Akiva 2018). In particular, to identify features that contribute to incident impacts, the interpretability of various models is used to confirm other important desiderata in ML systems. There are many auxiliary criteria that one may wish to optimize. Notions regarding fairness or unbiasedness imply that protected groups (explicit or implicit) are not discriminated against Doshi-Velez and Kim (2017). Generally, feature importance can be divided into modular global importance and local importance (Guidotti et al. 2018; Molnar 2020). While modular global feature importance measures the importance of a feature for an entire model, local importance measures the contribution of a feature to a specific observation. To reflect the uniqueness of an incident, we applied the LIME (Ribeiro, Singh, and Guestrin 2016) local interpretation methodology.

LIME interprets individual model predictions based on a local approximation of the model around a given prediction. We can evaluate how faithful a prediction is to the underlying model using LIME. One expectation is that our explanations should be locally accurate – meaning that in the vicinity of an input data point, our explanation should be faithful to the model (Lundberg and Lee 2017; Lipton 2018).

3. Definition of terminology

Consider a road network $\mathcal{G} = (V, E)$ as a directed connected graph, where V is a set of nodes representing road segments and E is the set of edges connecting those nodes. Let $v_i \in V$ denote a node and $e_{ij} = (v_i, v_j) \in E$ represent an edge. In the graph, we define in and out operators such that the operator $\text{in} : V \to 2^E$ returns all edges for which node v is the destination and the operator $\text{out} : V \to 2^E$ returns all edges whose source is node v. Additionally, $|\cdot|$ is defined as the number of set elements. For example, $|V|$ is the number of road segments in $\mathcal{G}$. Similarly, $|\text{in}(v)|$ is the number of road segments incoming to a node v, and $|\text{out}(v)|$ is the number of road segments outgoing from a node v.

Given a graph $\mathcal{G}$, we assume that the speed information of all road segments $v \in V$ is available at a predetermined time $t \in T$, which is denoted as $\{s(v, t) : V \times T \to \mathbb{R}^+\}$. Additionally, we let $s(v, T)$ denote a time series of speeds on road segment $v \in V$ during a predetermined period T. Because $s(v, T)$ is a vector, we can easily define quantities such as $\min(s(v, T))$, $\max(s(v, T))$, $\text{sum}(s(v, T))$, $\text{avg}(s(v, T))$, and $\text{sd}(s(v, T))$, where sd denotes standard deviation.

For further analysis, we define some basic terminology as follows.

Definition 3.1 (*k*-hop incoming (outgoing) neighbors): We define the k-nearest hops of the set of incoming nodes feeding traffic into a target node v_0, which are referred to as the k-hop incoming neighbors, as

$$N^k_{\text{in}}(v_0) := \bigcup_{v \in N^{k-1}_{\text{in}}(v_0)} \text{in}\,(v).$$

Similarly, we define the k-nearest hops of nodes taking traffic away from a target node v_0 through its out node, which are referred to as the k-hop outgoing neighbors, as

$$N^k_{\text{out}}(v_0) := \bigcup_{v \in N^{k-1}_{\text{out}}(v_0)} \text{out}\,(v).$$

Definition 3.2 (Incident-anchored subgraph): Given an incident road segment v_0, an incident-anchored subgraph $\mathcal{G}_{v_0} \subseteq \mathcal{G}$ is defined as a directed subgraph that connects an incoming subgraph of v_0, denoted as $\mathcal{G}^{(\text{in})}_{v_0} = (V^{(\text{in})}_{v_0}, E^{(\text{in})}_{v_0})$, and an outgoing subgraph of v_0, denoted as $\mathcal{G}^{(\text{out})}_{v_0} =$

$(V_{v_0}^{(\text{out})}, E_{v_0}^{(\text{out})})$, where

$$V_{v_0}^{(\text{in})} = \bigcup_{k=1}^{K} N_{\text{in}}^{k}(v_0), \quad V_{v_0}^{(\text{out})} = \bigcup_{k=1}^{K} N_{\text{out}}^{k}(v_0).$$

Definition 3.3 (Exponential moving average): Let $s(v,t)$ be the speed on traffic incident road segment v at time t. Then, *the exponential moving average* $\bar{s}(v,t)_n$ can be defined recursively as

$$\bar{s}(v,t)_n = \alpha \bar{s}(v,t-1)_n + (1-\alpha)s(v,t),$$

where n indicates the average period (Klinker 2011), and the weight factor α plays a role in controlling the importance of recent information. Although there are many possible choices for the weight factor, the most common choice is $\alpha = \frac{2}{n+1}$. The exponential moving average technique is typically applied to time series data to smooth short-term variations and capture long-term trends or cycles in the form of a moving average.

Definition 3.4 (Path, path set): Given a road network $\mathcal{G} = (V, E)$ with a set of nodes $V = \{v_1, \ldots, v_n\}$ and set of edges $E \subseteq V \times V$, a path in $\mathcal{G}$ is defined as a finite sequence

$$P = (v_0 e_{v_0} v_1 e_{v_1} \cdots v_{K-1} e_{v_{K-1}} v_K),$$

where $v_k \in V$ and $e_{v_k} = (v_k, v_{k+1}) \in E$ for all $k \in \{0, \ldots, K-1\}$. In a road network, a path is uniquely determined by its node sequence, and the notation can be simplified to

$$P = (v_0 v_1 v_2 \cdots v_K).$$

A path set in $\mathcal{G}$ is defined as a set of paths whose origin and length are identical in a road network. To specify the origin and length of a path, a path set is denoted as $P^K(v_0)$, where v_0 and K are the origin and length of the path, respectively.

The order of node sequences is opposite to the order of traffic flows.

Definition 3.5 (Congested, congestion indicator function): Given a node v, time duration T, and short period $[t-\delta : t] \in T$, a node v is said to be congested in T with δ if $\exists t \in T$ such that

$$\text{avg } s(v, [t-\tau : t]) < 0.6 \times ff(v), \tag{1}$$

where $ff(v)$ is the free-flow speed of road segment v. In this study, we used the maximum speed restriction as the free-flow speed.

Then, the congestion indicator function is defined as

$$c_\tau(v,T) = \begin{cases} 1, & \text{if a node } v \text{ is congested in } T \text{ with } \tau \\ 0, & \text{otherwise.} \end{cases}$$

There are several choices for the congestion thresholds in Equation (1). In this study, we adopted the value of 0.6 suggested by Basak, Dubey, and Bruno (2019) after consulting with domain experts. $\tau = 30$ (min) was assumed, and sensitivity analysis for τ was performed as discussed in Section 6.3. For notational simplicity, $c_\tau(v,T)$ is abbreviated as $c(v,T)$.

Definition 3.6 (Sequence of propagation indicators, propagation indicator function): Given a path $P = (v_0 v_1 v_2 \cdots v_K)$ in $\mathcal{G}$ and incident duration T_{v_0}, a sequence of propagation indicators is defined as a finite sequence

$$p\text{-seq}(P, T_{v_0}) = (q(v_1, T_{v_0}), q(v_2, T_{v_0}), \ldots, q(v_K, T_{v_0})),$$

where $q(v_i, T_{v_0})$ is the propagation indicator function. For a node v_i, let $t_{v_i}^{(1)}$ denote the first $t \in T_{v_0}$ that satisfies Equation (1). Assuming that $c(v_0, T_{v_0}) = 1$, the propagation indicator function is defined as

$$q(v_i, T_{v_0}) = \begin{cases} 1, & \text{if } c(v_i, T_{v_0}) = 1 \text{ and } c(v_{i-1}, T_{v_0}) = 1 \text{ and } t_{v_{i-1}}^{(1)} < t_{v_i}^{(1)} \\ 0, & \text{otherwise} \end{cases}$$

for $i \geq 1$. The propagation indicator is defined such that congestion propagation is considered to occur only when the connected incoming road of the currently congested road is congested during the next period.

Definition 3.7 (Reported time): After a nonrecurrent incident occurs on road segment v_0, the point at which information regarding the incident is released to the public is defined as $t_{v_0}^{(rpt)}$. In the case of a traffic incident, it is typically difficult to determine the time interval between when an incident occurs and $t_{v_0}^{(rpt)}$. For example, it is known that it takes approximately 15 min for information to be released after a traffic incident occurs in Seoul, South Korea.

4. Methodology

This section presents the problem statement and the three nonrecurrent congestion measures we propose to quantify incident impacts: incident duration, congestion propagation level, and speed drop ratio. In addition, we present the prediction models developed to extract meaningful information regarding influential features related to the proposed measures.

4.1. Problem statement

The aim of this study was to analyze the proposed measures and their association with temporal, spatial, topological, operational, and other environmental factors. These associated factors are called features. Consider N incident-anchored subgraphs $\mathcal{G}_i$, $i = 1, \ldots, N$. Let $\mathbf{X} \in \mathbb{R}^{N \times C}$ be a feature matrix of the subgraphs, where C is the number of features, and $\mathbf{y}^{(m)} = (y_1^{(m)}, \ldots, y_N^{(m)})^T \in \mathbb{R}^N$ represent a measure of traffic incident impacts. Then, we aim to train a function $f_m(\cdot)$ that maps a feature matrix $\mathbf{X}$ to $\mathbf{y}^{(m)}$ as follows:

$$\mathbf{X} \xrightarrow{f_m(\cdot)} \mathbf{y}^{(m)}.$$

Let $\hat{f}_m(\cdot)$ denote the trained function. We can predict the impact of a new incident, $\mathbf{y}_{new}^{(m)}$, by applying $\hat{f}_m(\mathbf{X}_{new})$, where $\mathbf{X}_{new}$ represents the features of the new incident.

4.2. Measuring nonrecurrent traffic congestion

Figure 1 illustrates the concepts underlying the three proposed measures. Figure 1(a) illustrates the concepts of incident duration and speed drop ratio, and Figure 1(b) illustrates the concept of congestion propagation to incoming neighbors, where incoming neighbors are incoming roads feeding traffic into the road at which the incident occurred. The black solid line represents the average speed of the road segment where a traffic incident occurs, while the orange, green, and blue solid lines represent the average speeds of the incoming neighbors.

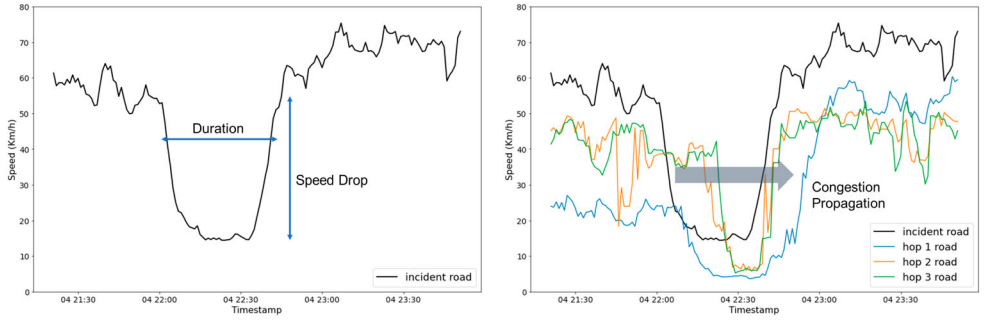

Figure 1. Concepts of the proposed nonrecurrent congestion measures. (a) Incident duration and speed drop ratio and (b) Congestion propagation level.

4.2.1. Incident duration

Many studies have been conducted on traffic incident duration analysis. (For further details, readers are referred to Ruimin Li, Pereira, and Ben-Akiva (2018) and references therein.) To calculate the duration of an incident, previous studies predominantly assumed that traffic incident occurrence and clearance information are available or that the probabilistic distribution of the duration is known. However, such assumptions may not be valid. To detect the incident duration using traffic speed data, Haule et al. (2019) used the lower bound of the historical speed profile and defined the incident duration as the period during which that speed was out of bounds. Unfortunately, this kind of approach is not applicable to our situation, because the high variability in trajectory-based average road speed can lead to numerous false positives in incident detection.

To address these challenges, we developed a simple rule-based approach in which the incident duration is calculated using trajectory-based average road speeds. Suppose that a traffic incident occurs on road segment v_0 and is reported at time $t_{v_0}^{(rpt)}$. To determine the incident duration, it is necessary to estimate the time at which the incident begins and ends. We assumed that the traffic incident will lead to dramatic changes in speed, pattern, and variation. Under this assumption, it is possible to estimate the incident start time as the time when such a dramatic change is first detected. Formally, the incident start time $t_{v_0}^{(st)}$ is estimated as

$$t_{v_0}^{(st)} = \min\{t : t \text{ satisfies } (C1), (C2), (C3)\}, \quad t = \ldots, t_{v_0}^{(rpt)} - 1,$$

where

$$(C1): \quad \bar{s}(v_0, t)_5 \leq s^{\mathrm{REG}}(v_0, t) \tag{2}$$

$$(C2): \quad \bar{s}(v_0, t)_5 \leq \bar{s}(v_0, t)_{30} \tag{3}$$

$$(C3): \quad s(v_0, t) \leq s(v_0, t-1) - \mathrm{sd}(s(v_0, [t-\delta : t]). \tag{4}$$

The first condition in Equation (2) indicates that the exponential moving average, $\bar{s}(v_0, t)_5$, should be less than the regular road speed. Exponential moving averages are used rather than direct road speeds because they are less volatile and show trends in speed patterns. $s^{\mathrm{REG}}(v_0, t)$ represents the regular road speed, which can be obtained either from historical road speed data or the average road speed for the preceding hours. Note that the regular road speed considers the influence of recurrent traffic congestion. In this study, we assume that $s^{\mathrm{REG}}(v_0, t)$ is given.

The second condition in Equation (3) is closely related to the concept of a death cross in stock chart analysis, and is used to capture short-term speed patterns (Ausloos and Ivanova 2002; Harish et al. 2019). It is known that a death cross appears on a chart when the moving average of the short-term stock price crosses the long-term moving average, indicating that the trend of recent price drops

is stronger than that of long-term price drops. We set the second condition to determine whether the short-term (5 min interval) speed trend overtakes the long-term (30 min interval) speed trend.

The final condition in Equation (4) sets a condition based on whether there is a radical speed drop. If a traffic incident occurs, the speed of the vehicles affected by the incident is expected to drop sharply after the incident. To reflect variations in the speed distribution, we detect a sharp speed drop if the speed decreases by more than its standard deviation $\mathrm{sd}(s(v_0, [t-\delta : t])$.

In contrast to estimating the incident start time, the incident recovery time is estimated as the time at which the dramatic change caused by the incident first returns to normal, where 'return to normal' is defined as the state in which the average speed for a certain period is higher than the regular road speed. Formally, the incident recovery time, $t_{v_0}^{(end)}$, is estimated as

$$t_{v_0}^{(end)} = \min\{t : s^{\mathrm{REG}}(v_0, t) < \mathrm{avg}\,(s(v_0, [t-\delta : t]))\}, \quad t = t_{v_0}^{(st)} + \delta + 1, \ldots. \tag{5}$$

In Equations (4) and (5), we set $\delta = 30$ (min). (Sensitivity analysis for δ is performed in Section 6.3.) Then, the incident duration ($y_{v_0}^{(1)}$) can be defined as

$$y_{v_0}^{(1)} := t_{v_0}^{(end)} - t_{v_0}^{(st)}. \tag{6}$$

The period $[t_{v_0}^{(st)} : t_{v_0}^{(end)}]$ is denoted as $T_{v_0}^{(1)}$. The length of $T_{v_0}^{(1)}$ is $y_{v_0}^{(1)}$.

4.2.2. Incident-driven congestion propagation level

Traffic congestion has been measured by the change in traffic flow, which is the multiplication of traffic density and average traffic speed (Wright and Roberg 1998; Ceulemans et al. 2009). However, as users of navigation services are not representative of the whole, in our case, only the trajectory-based speeds of users are available, rather than traffic density or flow data. Using trajectory-based average road speeds, we propose an incident-driven congestion propagation level measure.

Consider an incident-anchored subgraph, $\mathcal{G}_{v_0}$. Let P_w be the wth path of the subgraph to the incident road segment, where $w = 1, \ldots, W$. Because the incident-anchored subgraph considers up to K-hop incoming neighbors by Definition 3.1, each path consists of $K+1$ connected road segments, including the incident road segment v_0,

$$P_w = (v_0 v_1^w v_2^w \cdots v_K^w).$$

Given an incident duration $T_{v_0}^{(1)}$ from Equation (6), we can compute $q(v_k, T_{v_0}^{(1)})$ for $v_k \in P_w, k = 1, \ldots, K$, using the propagation indicator function defined in Definition 3.6. If $q(v_k, T_{v_0}^{(1)}) = 1$, it indicates that the congestion caused by the incident at v_0 propagates along the path to road segment v_k.

To quantify the impact of a traffic incident to incoming neighbors, we propose a new measure called the *incident-driven congestion propagation level*. Based on the number of lanes ($d(v)$) and length of the road segment ($\ell(v)$), the incident-driven congestion propagation level is defined as

$$y_{v_0}^{(2)} := \sum_{v \in V_{v_0}^{(\mathrm{in})}} q\left(v, T_{v_0}^{(1)}\right) \cdot d(v) \cdot \ell(v). \tag{7}$$

This level represents the weighted number of road segments where congestion propagated in the incident-anchored subgraph; the weights reflect the number of lanes and the length of the road segment. The larger the number of lanes, the longer the length of a road, and the more propagation in a subgraph, the larger $y_{v_0}^{(2)}$ becomes.

4.2.3. Incident-driven speed drop ratio

Measuring speed reduction is a natural way to quantify the impact of a traffic incident. In the literature, the speed reduction index (SRI) and speed performance index (SPI) are commonly used (Afrin and Yodo 2020). The SRI is the ratio of the relative speed change between congested and free-flow

conditions, whereas the SPI is the ratio of the relative speed change between the congested speed and the maximum permissible speed.

To quantify the impact of a traffic incident on speed reduction, we extend the concept of the SRI and SPI and propose a new measure called the *incident-driven speed drop ratio*. Given the time $t_{v_0}^{(rpt)}$ at which an incident is reported, the incident-driven speed drop ratio is defined as the ratio of the speeds before and after $t_{v_0}^{(rpt)}$. Formally,

$$y_{v_0}^{(3)} := \max\left(0, 1 - \frac{\min\left(s(v_0, [t_{v_0}^{(rpt)} : (t_{v_0}^{(rpt)} + t_{aft})])\right)}{\max\left(s(v_0, [(t_{v_0}^{(rpt)} - t_{bf}) : t_{v_0}^{(rpt)}])\right)}\right). \tag{8}$$

In this study, we set $t_{aft} = t_{bf} = 60$ under the assumption that the average speed drops sharply between 1 h before and 1 h after the incident reported time.

4.3. Model-based feature importance

LIME is a novel technique that can explain the predictions of any prediction model by training a local surrogate model (Ribeiro, Singh, and Guestrin 2016). Local surrogate models are interpretable models that can explain individual predictions from a prediction model. Suppose that f is a prediction model for predicting $\mathbf{y}$ and $\mathbf{y} = f(\mathbf{X})$, where $\mathbf{X}$ is a feature matrix. Here, it is assumed that we can probe the prediction model f as often as we wish. Let $g \in G$ be an explanation model, where G is a class of potentially interpretable models. Our goal is to use a local surrogate model to understand why the prediction model makes a certain prediction. LIME produces a local surrogate model using the following equation:

$$\xi(\mathbf{x}) = \text{argmin}_{g \in G} \mathcal{L}(f, g, \pi_{\mathbf{x}}) + \Omega(g), \tag{9}$$

where $\mathcal{L}$ is a measure of how unfaithfully g approximates f in the locality defined by $\pi_{\mathbf{x}}$, and $\Omega(g)$ is a measure of the complexity of the explanation $g \in G$. Here, we use the locally weighted square loss $\mathcal{L}$, exponential kernel $\pi_{\mathbf{x}}$, and complexity measure $\Omega(g)$, as defined in Ribeiro, Singh, and Guestrin (2016). To learn the local behavior of f, $\mathcal{L}$ is approximated by drawing samples weighted by $\pi_{\mathbf{x}}$. The samples are perturbed instances around $\mathbf{x}_i$ generated by adding random noise to local instances near $\mathbf{x}_i$. For an instance $\mathbf{x}_i$, we can obtain $\xi(\mathbf{x}_i)$ using Equation (9). Let $h_{i,j}$ be the coefficient corresponding to the jth feature in $\xi(\mathbf{x}_i)$. Then, the importance of the jth feature can be obtained as

$$I_j = \frac{\sum_{i=1}^{N} |h_{i,j}|}{N}, \tag{10}$$

where N is the number of incidents. To identify the relative contribution of each feature, the relative importance is defined as

$$RI_j = \frac{I_j}{\sum_{j=1}^{C} I_j}, \tag{11}$$

where C is the number of features.

Within the context of this study, we consider three separate prediction models, f_m, $m = 1, 2, 3$, for predicting the incident-driven measures, $\mathbf{y}^{(m)}$. That is, $\mathbf{y}^{(m)} = f_m(\mathbf{X})$, where $\mathbf{X} \in \mathbb{R}^{N \times C}$ is a feature matrix of the incident-anchored subgraphs for traffic incidents. Our goal is to train a prediction model $f_m(\cdot)$ that maps a feature matrix $\mathbf{X}$ to $\mathbf{y}^{(m)}$, and to understand why a prediction model makes a certain prediction using LIME. LIME uses the local surrogate model to identify important features using Equation (10). In this study, understanding which features are important for making a certain prediction is termed 'interpretability.'

Figure 2. Road network in Seoul where the case study incident occurred.

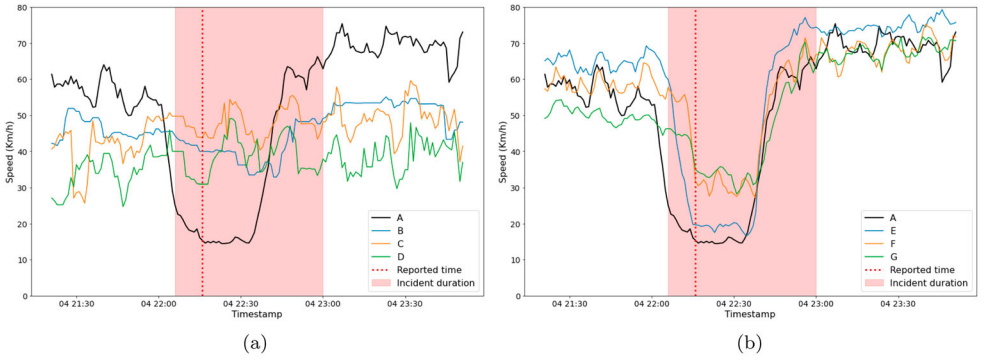

Figure 3. Speed patterns affected by nonrecurrent traffic congestion in Seoul. (a) Speed patterns of (A, B, C, D) and (b) Speed patterns of (A, E, F, G).

5. Case study: incident on Gangbyeonbuk-ro

The proposed nonrecurrent congestion measures were applied to a real incident case on Gangbyeonbuk-ro in Seoul. A traffic incident at the location shown in Figure 2 was reported at 22:16 on September 4, 2020. This road network is known to have high traffic volumes and complexity. The asterisk in the figure indicates the exact location at which the incident occurred, and the black line (A) indicates the road segment to which the location belongs. The red lines signify the *1*-hop incoming neighbors (B, H, E) of the incident road (A), and the blue and green lines signify the *2*-hop incoming neighbors (C, I, K, F) and *3*-hop incoming neighbors (D, J, L, M, G), respectively.

Traffic on road A has an impact on five different incoming paths within three hops. The five paths are $P_1 = (A, B, C, D), P_2 = (A, E, F, G), P_3 = (A, H, I, J), P_4 = (A, H, K, L)$, and $P_5 = (A, H, K, M)$. Figure 3(a,b) illustrate the speed patterns of P_1 and P_2, respectively. In the figures, the y axis represents the average speed value in km/h.

We applied the three proposed nonrecurrent congestion measures to the real incident case and obtained $y_A^{(1)}, y_A^{(2)}$, and $y_A^{(3)}$. First, the incident duration $y_A^{(1)}$ was computed to be 54 min, using Equation (6) with $t_A^{(st)} = 22{:}06$ and $t_A^{(end)} = 23{:}00$, as indicated by the red box in Figure 3. Results indicate that the incident was reported 10 min after it actually occurred, and conditions returned to normal 54 min later.

Next, given the period of the incident duration, $T_A^{(1)} = [22{:}06, 23{:}00]$, we calculated the propagation indicators for all road segments in the subgraph as follows:

$$
\begin{aligned}
&q\left(B, T_A^{(1)}\right) = 0, \quad q\left(C, T_A^{(1)}\right) = 0, \quad q\left(D, T_A^{(1)}\right) = 0\\
&q\left(E, T_A^{(1)}\right) = 1, \quad q\left(F, T_A^{(1)}\right) = 1, \quad q\left(G, T_A^{(1)}\right) = 1\\
&q\left(H, T_A^{(1)}\right) = 1, \quad q\left(I, T_A^{(1)}\right) = 1, \quad q\left(J, T_A^{(1)}\right) = 1\\
&q\left(K, T_A^{(1)}\right) = 1, \quad q\left(L, T_A^{(1)}\right) = 0, \quad q\left(M, T_A^{(1)}\right) = 0
\end{aligned}
$$

The results are congruent with Figure 3, in that $P_1 = (A, B, C, D)$ was not affected by the incident whereas the impact of the incident propagated along $P_2 = (A, E, F, G)$. The values of the propagation indicators show that the impacts propagated to seven road segments out of the 12 incoming roads of A. Consequently, we calculated the incident-driven congestion propagation level to be $y_A^{(2)} = 23.10$ using Equation (7). This value denotes the sum of the traffic capacity affected by a traffic incident in the incident-anchored subgraph.

Lastly, $y_A^{(3)}$ was computed to be 0.77 using Equation (8), based on

$$
\max\left(s(v_0, [(t_{v_0}^{(rpt)} - 60) : t_{v_0}^{(rpt)}])\right) = 63.99, \quad \min\left(s(v_0, [t_{v_0}^{(rpt)} : (t_{v_0}^{(rpt)} + 60)])\right) = 14.45.
$$

This means that the trajectory-based average road speed decreased by 77% after the incident reported time, relative to the speed before the incident reported time.

In summary, the computed values for the proposed nonrecurrent congestion measures of the incident were

$$
\left(y_A^{(1)}, y_A^{(2)}, y_A^{(3)}\right) = (54, 23.10, 0.77).
$$

These values not only quantify the impact of an incident, they also allow comparison with the impact of other incidents. For example, Figure 4 shows histograms of the three measures for 1322 incidents in Seoul, South Korea. (The data descriptions are presented in Section 6.1.) The red dotted lines in the figure indicate the position of the case incident among 1322 incidents in terms of incident impacts. The values of $(54, 23.10, 0.77)$ are respectively in the 33rd, 84th, and 80th percentile of the 1322 incidents by incident impact. The incident duration of the case incident was short, but the congestion propagation level and the speed drop ratio were larger.

6. Real data example: traffic incidents in Seoul

The proposed method was validated on 1425 real traffic incidents that occurred from September 2 to December 1, 2020, in Seoul, South Korea. Figure 5 shows the locations of the 1425 traffic incidents (black dots) considered in this study.

6.1. Datasets

Two types of datasets were considered from different sources: a traffic dataset provided by the NAVER corporation navigation team and an incident dataset provided by the Korean National Police Agency.

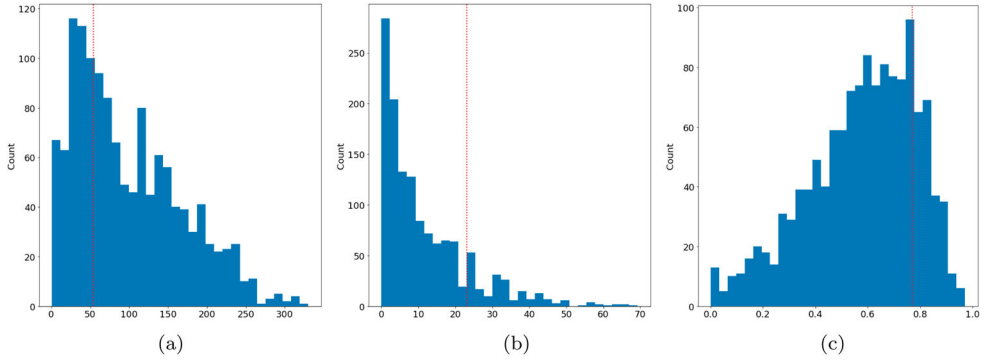

Figure 4. Histograms of incident duration, congestion propagation level, and speed drop ratio for 1322 incidents in Seoul, South Korea. (a) Incident duration. (b) Congestion propagation level and (c) Speed drop ratio.

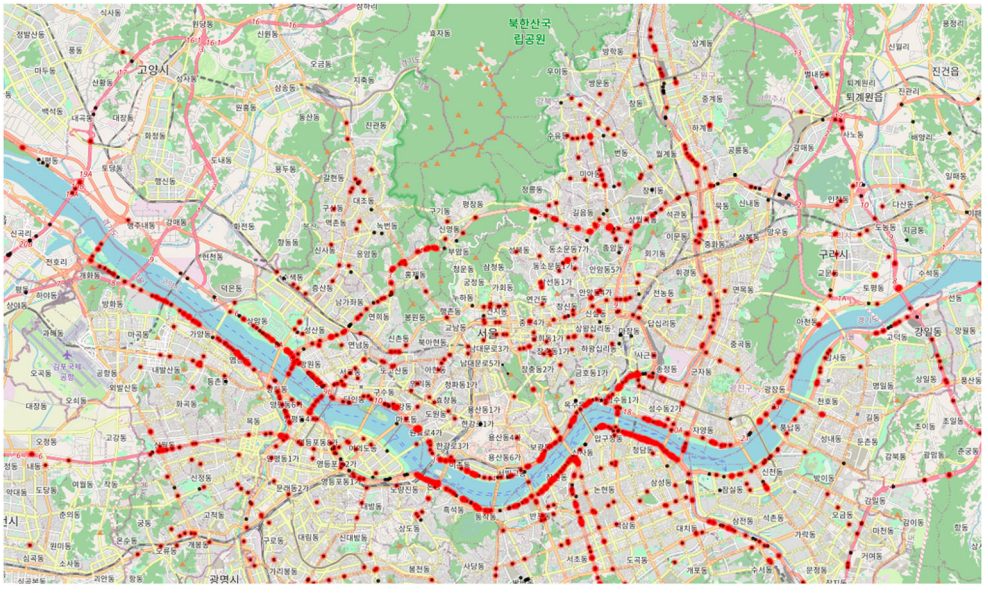

Figure 5. Locations of traffic incidents in Seoul from September 1, 2020 to December 1, 2020 (red dots indicate the selected incidents).

The traffic dataset consists of a traffic road network with trajectory-based speed, weather, and road attributes of the major metropolitan area of Seoul, where nearly half of the country's population resides. The speed data are described by GPS trajectories. A GPS trajectory consists of a series of points with latitude, longitude, and timestamp information generated when navigation service users travel. To align a sequence of observed user positions with the road network, we used a map-matching process (Newson and Krumm 2009).

The incident dataset provided by the Korean National Police Agency contains 1425 incidents that occurred during the aforementioned period in Seoul. Each incident record includes the reported time, description of the incident, and originating location described by both geographical coordinates and road segment ID.

For validation purposes, we selected 1322 of the 1425 incidents, each with an incident duration greater than zero. The selected incidents are represented by the red dots in Figure 5. Consequently,

Table 1. Description of independent features.

Categories	Features	Value set & Description
Timestamp	time of day	1: $0 \leq$ incident time < 6 2: $6 \leq$ incident time < 12 3: $12 \leq$ incident time < 18 4: $18 \leq$ incident time < 24
	day of week	0: weekday 1: weekend (Saturday or Sunday)
Road Characteristics	road type	1: highway 2: urban highway 3: general national road 4: state-sponsored regional road 5: local road 6: general road
	incident road speed limit	$30 \leq s_{\max}(v_0) < 120$
	incident road length	length of the road segment where the incident occurred
	number of lanes	number of lanes of an incident road
Network topology	number of incoming roads	$\lvert V_{v_0}^{(\text{in})} \rvert$
	number of outgoing roads	$\lvert V_{v_0}^{(\text{out})} \rvert$
	in-degree centrality	Cd_{in}
	out-degree centrality	Cd_{out}
	closeness centrality	Cc
	betweenness centrality	Cb
	eigenvector centrality	Ce
Speed	incoming correlation	$\text{corr}_{\text{in}}(v_0)$
	outgoing correlation	$\text{corr}_{\text{out}}(v_0)$
	prior speed drop ratio	$0 \leq psdr \leq 1$
	speed variation	standard deviation of speed data prior to incident occurrence
Source	information source	1: traffic broadcasting 2: national transport information center 3: police station 4: infrastructure and transport
Weather	weather code	0: clear weather (sunny) 1: cloudy 2. rain
	rain amount	rain amount
	rain probability	probability of rain
	temperature	temperature

this study considered 1322 incident-anchored subgraphs $\mathcal{G}_{v_{0,i}}$, $i = 1, 2, \ldots, 1322$. This corresponds to 34,195 road segments where $K = 3$.

6.2. Independent features

Table 1 summarizes the key independent features extracted from both the traffic dataset and incident dataset for the incident-anchored subgraphs. The extracted features can be categorized as follows: Timestamp, Road Characteristics, Network Topology, Speed, Source, and Weather.

(1) *Timestamp*: Two features are considered: 'time of day' and 'day of week.' The former represents daily patterns, and the latter represents weekly patterns.
(2) *Road Characteristics*: Road characteristics and its related features include 'road type,' 'incident road speed limit,' 'incident road length,' and 'number of lanes.' 'incident road length' and 'number of lanes' respectively represent the geographical length and width of the road segment on which an incident occurs.
(3) *Network Topology*: The topological features of the road network include 'number of incoming roads,' 'number of outgoing roads,' 'in-degree centrality,' 'out-degree centrality,' 'closeness centrality,' 'betweenness centrality,' and 'eigenvector centrality.'In this study, we modified 'degree

centrality,' which is a well-known node complexity measure in an undirected network (Freeman 1978; Zhang and Luo 2017; Saxena, Malik, and Iyengar 2016), to measure node complexity in a directed network. Let us denote the node complexity on the side of the incoming nodes by 'in-degree centrality' (Cd_{in}) and on the side of the outgoing nodes by 'out-degree centrality' (Cd_{out}) in an incident-anchored subgraph:

$$Cd_{\text{in}} = \frac{|\text{in}(v_0)|}{|V_{v_0}|}, \quad Cd_{\text{out}} = \frac{|\text{out}(v_0)|}{|V_{v_0}|}.$$

The 'closeness centrality' (Cc) of a road segment v_0 is the reciprocal of the sum of the shortest path distances from v_0 to all other road segments in the subgraph (Freeman 1977; Newman 2008). Because the sum of the distances depends on the number of road segments in the subgraph centered around v_0, the closeness is normalized relative to the sum of the minimum possible distances $|V_{v_0}| - 1$ as follows:

$$Cc = \frac{|V_{v_0}| - 1}{\sum_{v_i \in V_{v_0}} d(v_i, v_0)},$$

where $d(v_i, v_0)$ is the shortest path distance between $v_i \in V_{v_0}$ and v_0.

'Betweenness centrality' (Cb) quantifies the number of times a road functions as a bridge along the shortest path between two other roads (Freeman 1977; Newman 2008). It reflects the amount of influence a road has on the flow of information in a graph. The 'betweenness centrality' of a road v_0 in our problem setting is the sum of the fractions of all pairs of shortest paths that pass through v_0.

$$Cb = \sum_{v,v' \in V_{v_0}} \frac{\sigma(v, v'|v_0)}{\sigma(v, v')},$$

where $\sigma(v, v')$ is the total number of shortest paths from road v to v' and $\sigma(v, v'|v_0)$ is the number of paths that pass through v_0. Therefore, the greater the value of Cb, the higher the probability that v_0 is located in the middle of the shortest paths connecting two other roads.

'Eigenvector centrality' (Ce), on which Google's PageRank is based (Zaki, Meira, and Meira 2014), measures the influence of a node in a network (Freeman 1977; Newman 2008). Let $A = (a_{i,j})$ be the adjacency matrix of a subgraph. The Ce of node v_0 is given by

$$Ce_{v_0} = \frac{1}{\lambda} \sum_{v \in V_{v_0}} a_{v,v_0} Ce_v,$$

where $\lambda \neq 0$ is a constant. In matrix form, we have $\lambda Ce = CeA$.

(4) *Speed*: When an incident occurs, the traffic flow between the incident road and neighboring roads can be positively or negatively correlated. To measure such correlations, we define the incoming correlation ($\text{corr}_{\text{in}}(v_0)$) and outgoing correlation ($\text{corr}_{\text{out}}(v_0)$) as

$$\text{corr}_{\text{in}}(v_0) = \frac{1}{\left|V_{v_0}^{(\text{in})}\right|} \sum_{v_j \in V_{v_0}^{(\text{in})}} \rho_{T_{v_0}^{(1)}}(v_0, v_j)$$

$$\text{corr}_{\text{out}}(v_0) = \frac{1}{\left|V_{v_0}^{(\text{out})}\right|} \sum_{v_j \in V_{v_0}^{(\text{out})}} \rho_{T_{v_0}^{(1)}}(v_0, v_j),$$

where $\rho_T(v_A, v_B)$ is the correlation coefficient of the two time series $s(v_A, T)$ and $s(v_B, T)$. 'Prior speed drop ratio' (*psdr*) is another speed-related independent feature. It measures the degree of

Table 2. Description of the hyper-parameters used in sensitivity analysis.

Measures	Hyper-parameters	Default (min)	Changes (min)
Incident duration	Average period (short) in Equation (3)	5	5, 10, 15
Incident duration	Average period (long) in Equation (3)	30	20, 30, 40
Incident duration	δ in Equation (4)	30	[10, 50]
Congestion propagation level	τ in Definition 3.5	30	[10, 50]
Speed drop ratio	t_{bf} in Equation (8)	60	[40, 80]

Table 3. Incident duration for the hyper-parameter changes in an average period.

		Average period (long)		
		20	30	40
Average period (short)	5	91.17	91.30	91.27
	10	87.25	87.42	87.01
	15	86.07	85.37	85.02

a speed drop over t_{bf} prior to an incident as

$$psdr := 1 - \frac{\min\left(s(v_0, [(t_{v_0}^{(rpt)} - t_{bf}) : t_{v_0}^{(rpt)}])\right)}{\max\left(s(v_0, [(t_{v_0}^{(rpt)} - t_{bf}) : t_{v_0}^{(rpt)}])\right)}.$$

In addition, we consider the standard deviation of $s(v_0, [(t_{v_0}^{(rpt)} - t_{bf}) : t_{v_0}^{(rpt)}])$ to measure the variability of speed data prior to incident occurrence.

(5) *Source*: We consider the source of an incident report as an operational feature. Depending on the party detecting an incident, the time required to clean up the incident scene may vary (Park, Haghani, and Zhang 2016). In our data, there were four report sources: traffic broadcasting, police stations, national transport information centers, and infrastructure and transport authorities.

(6) *Weather*: Weather may have an impact on incident duration. We considered 'weather code,' 'rain amount,' 'rain probability,' and 'temperature' in this study.

6.3. Sensitivity analysis

To validate the robustness of the three proposed measures with respect to hyper-parameter changes, we performed a sensitivity analysis for different hyper-parameter values and analyzed the relative changes of the proposed measures. The relative changes of the proposed measures were calculated for differences in the hyper-parameter from the default values. The default values were determined by domain experts.

Table 2 shows the experimental settings for the sensitivity analysis. For the incident duration, we used two exponential moving averages to detect the incident start time. In Definition 3.3, exponential moving average requires a hyper-parameter for an average period. Accordingly, two hyper-parameters are used: one is for an exponential moving average with short-term speed patterns and the other is for an exponential moving average with long-term speed patterns. In this sensitivity analysis, we considered various hyper-parameter values for the average periods: 5, 10, 15 min for short-term speed patterns and 20, 30, 40 min for long-term speed patterns. In addition, we considered changes from the default values for other hyper-parameters, such as δ for the incident duration, τ for the congestion propagation level, and t_{bf} for the speed drop ratio, as shown in Table 2.

Table 3 shows the average duration of 1322 incidents for different combinations of two average period lengths. The average incident duration does not change significantly for the changes in the average period lengths.

Figure 6 shows the relative change of each measure according to the various hyper-parameter values. The *x*-axis represents the difference of the hyper-parameter value from the default value and

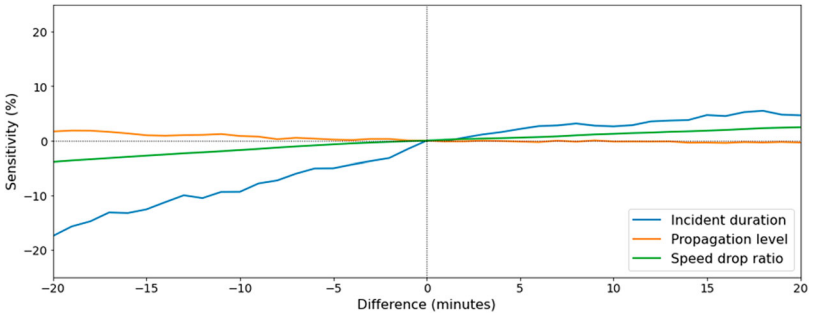

Figure 6. Relative changes of the three measures according to changes in hyper-parameters δ, τ, and t_{bf}.

Table 4. Performance comparisons of prediction models in terms of MAPE.

	Incident duration	Congestion propagation level	Speed drop ratio
LR	0.956	1.127	0.305
LASSO	0.933	1.028	0.364
Ridge	0.954	1.105	**0.304**
SVR	**0.808**	0.813	0.311
DT	1.055	**0.548**	0.383
RF	0.900	1.134	0.311
XGBoost	0.950	0.854	0.328
CatBoost	0.843	0.897	0.316
LGBM	0.894	0.831	0.306
MLP	0.937	1.324	0.332
Ensemble	0.873	0.820	0.325

the *y*-axis indicates the relative changes of the proposed measures. In general, the results confirm the robustness of the proposed measures with respect to hyper-parameter changes, but it is recommended that the value of δ in the incident duration ($y^{(1)}$) be at least 30 min. Otherwise, $\mathrm{sd}(s(v_0, [t-\delta : t])$ will fluctuate too much to detect the incident start time in a reliable manner.

6.4. Identifying influential features for traffic incident impacts

Suppose that f_m is a prediction model for predicting $\mathbf{y}^{(m)}$, $m = 1, 2, 3$, and $\mathbf{y}^{(m)} = f_m(\mathbf{X})$, where $\mathbf{X}$ is a feature matrix containing the independent features in Table 1 for 1322 traffic incidents. These independent features are normalized and used as prediction model features.

We used linear regression (LR), LASSO, ridge regression (Ridge), a support vector machine with a radial basis function kernel (SVR), decision tree (DT), random forest (RF), XGBoost, CatBoost, LGBM, and multilayer perceptron (MLP) as prediction models. To achieve robust prediction performance, we constructed individual ensemble models f_m, $m = 1, 2, 3$ from the three best-performing prediction models in terms of mean absolute percentage error (MAPE), as shown in Table 4. The incident data instances were divided into 1200 used for training and 122 for testing. To achieve robustness and generalization, we performed 10-fold cross validation and selected the best-performing model for each prediction model.

As a class of interpretable surrogate models *G*, we selected ridge regression models, which is the default class suggested by Ribeiro, Singh, and Guestrin (2016). Recall that our goal is to understand why a prediction model makes a certain prediction, using a local surrogate model according to Equation (9). By using the local surrogate model generated by LIME, we can identify important features using Equation (10). Figure 7 and Table 5 present the importance (I_j) and the relative importance (RI_j) of each feature in terms of the incident duration, congestion propagation level, and speed drop ratio. To

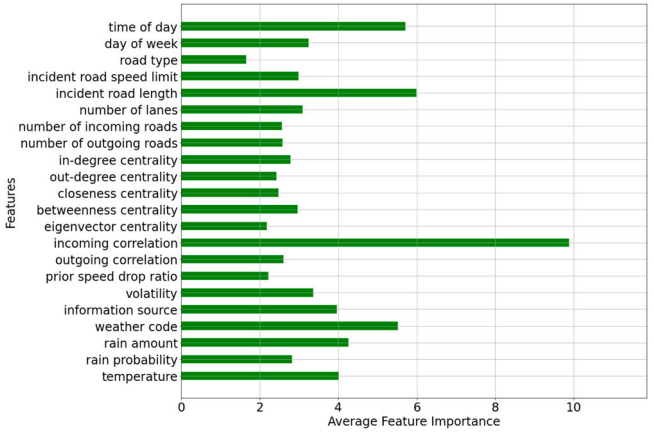

(a)

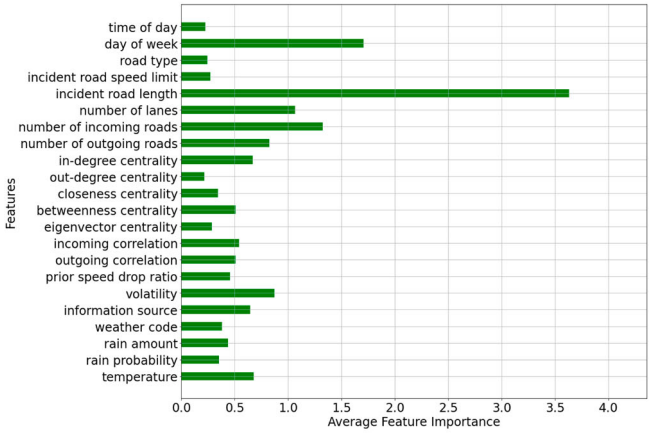

(b)

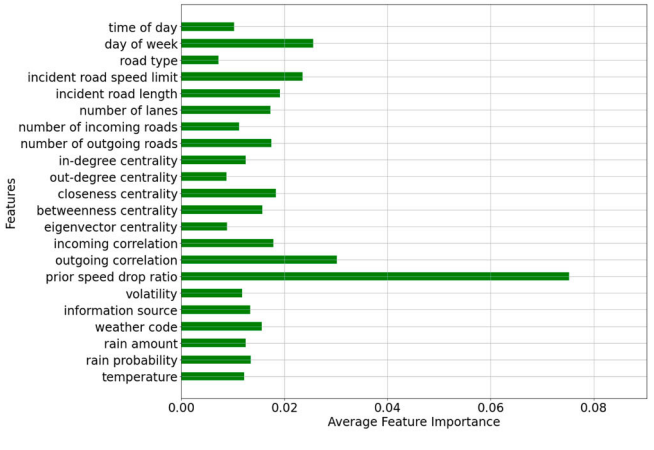

(c)

Figure 7. Comparison of feature importance in terms of influence on incident duration, propagation level, and speed drop ratio. (a) Feature importance for incident duration. (b) Feature importance for propagation level and (c) Feature importance for speed drop ratio.

Table 5. Results of LIME for feature importance.

		Incident duration		Congestion propagation level		Speed drop ratio	
Categories	Features	I_j	RI_j(%)	I_j	RI_j(%)	I_j	RI_j(%)
Timestamp	time of day	5.716	7.21	0.225	1.39	0.010	2.57
	day of week	3.249	4.10	1.705	10.53	0.026	6.44
Road characteristics	road type	1.649	2.08	0.246	1.52	0.007	1.82
	incident road speed limit	2.983	3.76	0.274	1.69	0.024	5.92
	incident road length	5.998	7.56	**3.630**	**22.42**	0.019	4.80
	number of lanes	3.090	3.90	1.067	6.59	0.017	4.35
Network topology	number of incoming roads	2.560	3.23	1.324	8.17	0.011	2.81
	number of outgoing roads	2.577	3.25	0.825	5.10	0.017	4.38
	in-degree centrality	2.788	3.52	0.670	4.14	0.012	3.13
	out-degree centrality	2.429	3.06	0.218	1.35	0.009	2.22
	closeness centrality	2.471	3.12	0.345	2.13	0.018	4.60
	betweenness centrality	2.965	3.74	0.506	3.13	0.016	3.95
	eigenvector centrality	2.184	2.75	0.286	1.77	0.009	2.22
Speed	incoming correlation	**9.880**	**12.46**	0.540	3.34	0.018	4.48
	outgoing correlation	2.601	3.28	0.506	3.13	0.030	7.58
	prior speed drop ratio	2.217	2.80	0.456	2.82	**0.075**	**18.89**
	volatility	3.366	4.24	0.873	5.39	0.012	2.96
Source	information source	3.969	5.00	0.647	3.99	0.013	3.37
Weather	weather code	5.517	6.96	0.382	2.36	0.016	3.93
	rain amount	4.257	5.37	0.438	2.71	0.013	3.14
	rain probability	2.820	3.56	0.351	2.17	0.013	3.39
	temperature	4.015	5.06	0.677	4.18	0.012	3.06

calculate I_j and RI_j, 30 perturbed instances were generated for each incident data instance to train the local surrogate model.

For the incident duration, 'incoming correlation' contributes the most, with relative importance of 12.46%. 'Incident road length' also contributes with 7.56% relative importance. These features are highly related to the traffic capacity of incident roads and inflow traffic volume. Compared with the outgoing road, inflow has more effect on the duration speed drop caused by the incident. In addition, weather code, which is an environmental incident factor, affects the duration with a relative importance of 6.96%.

For the congestion propagation level, 'incident road length' contributes the most with a relative importance of 22.42%, whereas 'number of lanes' contributes 6.59%. Interestingly, this means that the length of the incident road has a greater influence on our congestion propagation level than the width. Further, 'number of incoming roads' is a more important feature than 'number of outgoing roads.' This is logical because congestion propagates onto the incoming roads.

For the speed drop ratio, 'prior speed drop ratio' is the most important feature, with 18.89% relative importance. This result appears obvious, but we would like to note that all independent features, including 'prior speed drop ratio,' are available at the time of incident reporting. Therefore, 'prior speed drop ratio' can be used as an important feature in predictive models.

Furthermore, individual local surrogate models in LIME were used to investigate the dynamics of feature contributions according to the values of the incident impact measures. To determine how the importance changes according to the values of each measurement, Figure 8 compares the average importance values of two groups, respectively containing incidents having the five largest and five smallest values for each measure. For the incident duration and congestion propagation level, the difference in the average importance between the two groups is negligible, as shown in Figure 8(a,b). However, for the speed-drop ratio, Figure 8(c) reveals that the average importance values between the two groups exhibit significant differences. For example, 'prior speed drop ratio' has significantly different levels of importance between the two groups. This is reasonable because 'prior speed drop ratio' affects incidents with a large speed drop ratio more than those with a small speed drop ratio.

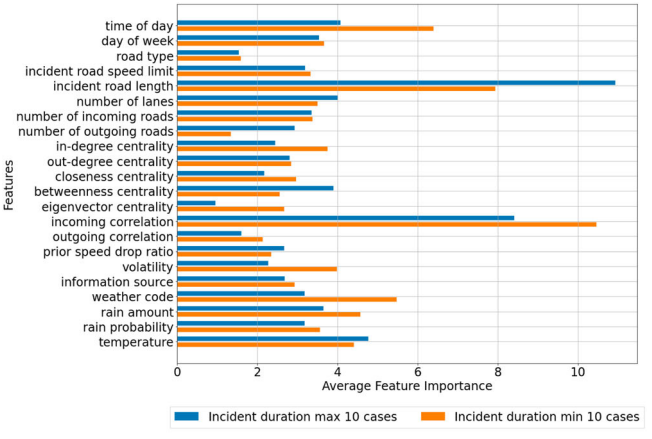

(a)

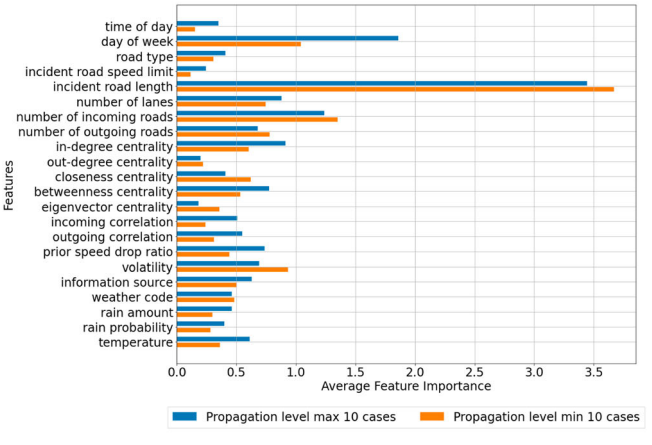

(b)

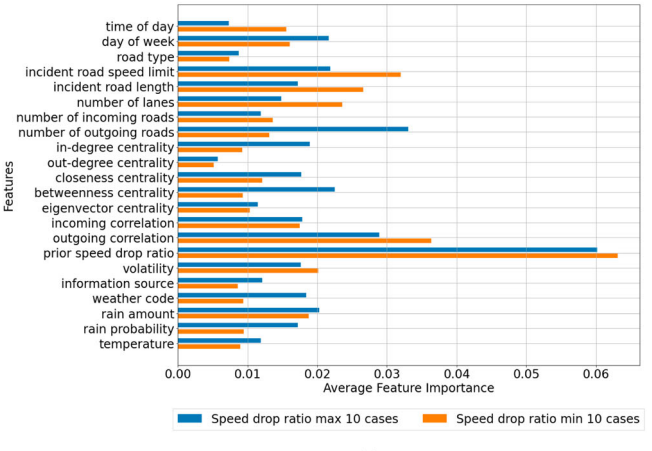

(c)

Figure 8. Comparison of the average importance values between groups of incidents with the five largest and five smallest values. (a) Feature importance for incident duration. (b) Feature importance for propagation level and (c) Feature importance for speed drop ratio.

Overall, the local interpretability of LIME enabled us to analyze feature importance at the individual traffic incident level.

7. Conclusion and discussion

Identifying various aspects of incident impacts and obtaining prior knowledge regarding the critical features contributing to each aspect are important tasks for both traffic operators and any corporation that provides navigation services. Completing these tasks can reduce the influence of an incident and provide drivers with alternative routes in real time. In this study, we proposed a new methodology to quantify incident impacts according to spatial, temporal, and speed aspects, and acquired reasonable feature importance values contributing to each aspect by applying a method called LIME to real traffic incident cases in Seoul, South Korea.

However, some limitations exist involving the data used in this study. First, the data may contain noise caused by different drivers, and it is difficult to define a purpose for each trajectory route (Choi et al. 2020; Kan et al. 2019). Second, the data collected from the navigation service are user-based; thus, they may not be representative of the traffic conditions on every road segment (Kan et al. 2019). In the case of narrow alleys, there are many NaN values because the amount of trajectory data from users traveling on such roads is insufficient and unreliable. Third, there is a lack of independent features that explain the uniqueness of traffic incidents, such as the number of casualties or injuries, number of vehicles involved, or number of lanes blocked. These are important independent features that distinguish traffic incidents and have a close relationship with the resulting incident impacts (Park, Haghani, and Zhang 2016). If more detailed incident data and precise speed data can be obtained, more accurate prediction of incident impacts and more precise interpretation of the related feature importance values should be possible, which would aid in the development of traffic plans for mitigating the adverse effects of traffic incidents.

Model transferability is an important issue. The proposed prediction models are transferable in terms of model forms (such as linear regression and ridge regression). However, attempting to transfer the estimated model from another urban region is not recommended, because the model parameters were estimated directly using local traffic data. Incident impacts on traffic vary from place to place, as they are a function of local conditions. Unlike other engineering models, transportation models are known to be highly sensitive to local conditions (Rossi, Bhat, et al. 2014). For example, the model parameters estimated using traffic data from Seoul cannot be used to predict the impacts of an incident in New York. Therefore, the proposed approach is not recommended for spatial extrapolation.

Future research must consider complex situations that may occur in actual incident situations. First, there may be secondary effects of congestion propagation. Drivers may select detour routes in response to incidents, creating new areas of congestion. Second, if an incident occurs under recurrent severe congestion, the reliability of the proposed measures is reduced because the impact of the incident can be offset. For example, the proposed measures may overestimate the incident duration by not detecting the incident or estimating the incident recovery time to be later than it actually is. Consequently, applicability of the proposed method can be limited to incidents that induced serious congestion, such as cascading incidents. Future work could include the development of nonrecurrent congestion measures for such complex situations.

Disclosure statement

No potential conflict of interest was reported by the author(s).

Funding

This work was partly supported by NAVER Corp. and Institute of Information & communications Technology Planning & Evaluation (IITP) grant funded by the Korea government (MSIT) (No.2020-0-01336, Artificial Intelligence Graduate School Program (UNIST)).

ORCID

JuYeong Lee http://orcid.org/0000-0002-4619-925X
Jiln Kwak http://orcid.org/0000-0002-8631-657X
YongKyung Oh http://orcid.org/0000-0002-8027-3433
Sungil Kim http://orcid.org/0000-0003-0208-4378

References

Afrin, Tanzina, and Nita Yodo. 2020. "A Survey of Road Traffic Congestion Measures Towards a Sustainable and Resilient Transportation System." *Sustainability* 12 (11): 4660.
Al-Deek, H., A. Garib, and A. E. Radwan. 1995. "New Method for Estimating Freeway Incident Congestion." *Transportation Research Record* (1494): 30–39.
Ausloos, M., and K. Ivanova. 2002. "Mechanistic Approach to Generalized Technical Analysis of Share Prices and Stock Market Indices." *The European Physical Journal B-Condensed Matter and Complex Systems* 27 (2): 177–187.
Basak, Sanchita, Abhishek Dubey, and Leao Bruno. 2019. "Analyzing the Cascading Effect of Traffic Congestion Using LSTM Networks." In *2019 IEEE International Conference on Big Data (Big Data)*, 2144–2153. IEEE.
Bennett, D. Scott. 1999. "Parametric Models, Duration Dependence, and Time-varying Data Revisited." *American Journal of Political Science* 43: 256–270.
Breslow, Norman E. 1975. "Analysis of Survival Data Under the Proportional Hazards Model." *International Statistical Review/Revue Internationale de Statistique* 43: 45–57.
Ceulemans, Wesley, Magd A. Wahab, Kurt De Proft, and Geert Wets. 2009. "Modelling Traffic Flow with Constant Speed Using the Galerkin Finite Element Method." In *Proceedings of the World Congress on Engineering*, Vol. 2. Citeseer.
Choi, Jaeheon, Kyuil Lee, Hyunmyung Kim, Sunghi An, and Daisik Nam. 2020. "Classification of Inter-urban Highway Drivers' Resting Behavior for Advanced Driver-assistance System Technologies Using Vehicle Trajectory Data From Car Navigation Systems." *Sustainability* 12 (15): 5936.
Chow, We-Min. 1976. "A Study of Traffic Performance Models Under An Incident Condition." *Transportation Research Record* 567: 31–36.
Chung, Younshik. 2010. "Development of An Accident Duration Prediction Model on the Korean Freeway Systems." *Accident Analysis & Prevention* 42 (1): 282–289.
Chung, Younshik, and Wilfred W. Recker. 2012. "A Methodological Approach for Estimating Temporal and Spatial Extent of Delays Caused by Freeway Accidents." *IEEE Transactions on Intelligent Transportation Systems* 13 (3): 1454–1461.
Chung, Younshik, and Byoung-Jo Yoon. 2012. "Analytical Method to Estimate Accident Duration Using Archived Speed Profile and Its Statistical Analysis." *KSCE Journal of Civil Engineering* 16 (6): 1064–1070.
Daganzo, Carlos F. 1994. "The Cell Transmission Model: A Dynamic Representation of Highway Traffic Consistent with the Hydrodynamic Theory." *Transportation Research Part B: Methodological* 28 (4): 269–287.
Doshi-Velez, Finale, and Been Kim. 2017. "Towards a Rigorous Science of Interpretable Machine Learning." Preprint. arXiv:1702.08608.
Freeman, Linton C. 1977. "A Set of Measures of Centrality Based on Betweenness." *Sociometry* 40: 35–41.
Freeman, Linton C. 1978. "Centrality in Social Networks Conceptual Clarification." *Social Networks* 1 (3): 215–239.
Garib, A., A. E. Radwan, and HJJoTE Al-Deek. 1997. "Estimating Magnitude and Duration of Incident Delays." *Journal of Transportation Engineering* 123 (6): 459–466.
Ghosh, Indrajit, Peter T. Savolainen, and Timothy J. Gates. 2014. "Examination of Factors Affecting Freeway Incident Clearance Times: a Comparison of the Generalized F Model and Several Alternative Nested Models." *Journal of Advanced Transportation* 48 (6): 471–485.
Goolsby, Merrell E. 1971. *Influence of Incidents on Freeway Quality of Service*. Highway Research Record 349.
Guidotti, Riccardo, Anna Monreale, Salvatore Ruggieri, Franco Turini, Fosca Giannotti, and Dino Pedreschi. 2018. "A Survey of Methods for Explaining Black Box Models." *ACM Computing Surveys (CSUR)* 51 (5): 1–42.
Haghani, A., D. Iliescu, M. Hamedi, and S. Yong. 2006. "Methodology for Quantifying the Cost Effectiveness of Freeway Service Patrols Programs–Case Study: HELP Program, i-95 Corridor Coalition." *Univ. of Maryland, College Park, MD*.
Hall, Randolph W. 1993. "Non-recurrent Congestion: How Big is the Problem? Are Traveler Information Systems the Solution?" *Transportation Research Part C: Emerging Technologies* 1 (1): 89–103.
Harish, Noor Ainy, S. K. Mohd Hairullah, S. Abu Bakar, and K. A. Abd Rahman. 2019. "Fuzzy Golden Cross and Fuzzy Death Cross As Stock Market Forecasting Indicator." *ASM Science Journal* 12 (Specia): 120–124.
Haule, Henrick J., Thobias Sando, Richard Lentz, Ching-Hua Chuan, and Priyanka Alluri. 2019. "Evaluating the Impact and Clearance Duration of Freeway Incidents." *International Journal of Transportation Science and Technology* 8 (1): 13–24.
He, Feifei, Xuedong Yan, Yang Liu, and Lu Ma. 2016. "A Traffic Congestion Assessment Method for Urban Road Networks Based on Speed Performance Index." *Procedia Engineering* 137: 425–433.
Highway Capacity Manual. 1994. TRB Special Report 209. Washington, DC: National Research Council.

Hojati, Ahmad Tavassoli, Luis Ferreira, Simon Washington, and Phil Charles. 2013. "Hazard Based Models for Freeway Traffic Incident Duration." *Accident Analysis & Prevention* 52: 171–181.

Hurdle, V. F., Mark I. Merlo, and Doug Robertson. 1997. "Study of Speed-flow Relationships on Individual Freeway Lanes." *Transportation Research Record* 1591 (1): 7–13.

Ji, Yangbeibei, Xiaoning Zhang, Winnie Daamen, and Lijun Sun. 2009. "Traffic Incident Recovery Time Prediction Model Based on Cell Transmission Model." In *2009 12th International IEEE Conference on Intelligent Transportation Systems*, 1–4. IEEE.

Ji, Yangbeibei, Xiaoning Zhang, and Lijun Sun. 2011. "Estimation of Traffic Incident Delay and its Impact Analysis Based on Cell Transmission Model." In *2011 IEEE Intelligent Vehicles Symposium (IV)*, 54–59. IEEE.

Kan, Zihan, Luliang Tang, Mei-Po Kwan, Chang Ren, Dong Liu, and Qingquan Li. 2019. "Traffic Congestion Analysis At the Turn Level Using Taxis' GPS Trajectory Data." *Computers, Environment and Urban Systems* 74: 229–243.

Karlaftis, Matthew G., and Eleni I. Vlahogianni. 2011. "Statistical Methods Versus Neural Networks in Transportation Research: Differences, Similarities and Some Insights." *Transportation Research Part C: Emerging Technologies* 19 (3): 387–399.

Khattak, Asad J., Joseph L. Schofer, and Mu-Han Wang. 1994. "A Simple Time Sequential Procedure for Predicting Freeway Incident Duration: IVHS Journal."

Klinker, Frank. 2011. "Exponential Moving Average Versus Moving Exponential Average." *Mathematische Semesterberichte* 58 (1): 97–107.

Lee, Jung-Taek, and Joseph Fazio. 2005. "Influential Factors in Freeway Crash Response and Clearance Times by Emergency Management Services in Peak Periods." *Traffic Injury Prevention* 6 (4): 331–339.

Li, Chi-Sen, and Mu-Chen Chen. 2014. "A Data Mining Based Approach for Travel Time Prediction in Freeway with Non-recurrent Congestion." *Neurocomputing* 133: 74–83.

Li, Yaping, Jian Lu, HongWu Li, Huihui Xiao, and Qingchao Liu. 2015. "An Approach to Modeling the Impact of Traffic Incident on Urban Expressway." *Discrete Dynamics in Nature and Society* 2015: Article 605016.

Li, Ruimin, Francisco C. Pereira, and Moshe E. Ben-Akiva. 2018. "Overview of Traffic Incident Duration Analysis and Prediction." *European Transport Research Review* 10 (2): 1–13.

Lipton, Zachary C. 2018. "The Mythos of Model Interpretability: In Machine Learning, the Concept of Interpretability is Both Important and Slippery." *Queue* 16 (3): 31–57.

Lundberg, Scott, and Su-In Lee. 2017. "A Unified Approach to Interpreting Model Predictions." Preprint. arXiv:1705.07874.

Molnar, Christoph. 2020. *Interpretable Machine Learning*. Lulu.com.

Nam, Doohee, and Fred Mannering. 2000. "An Exploratory Hazard-based Analysis of Highway Incident Duration." *Transportation Research Part A: Policy and Practice* 34 (2): 85–102.

Newman, Mark E. J. 2008. "The Mathematics of Networks." *The New Palgrave Encyclopedia of Economics* 2 (2008): 1–12.

Newson, Paul, and John Krumm. 2009. "Hidden Markov Map Matching Through Noise and Sparseness." In *Proceedings of the 17th ACM SIGSPATIAL International Conference on Advances in Geographic Information Systems*, (ACM SIGSPATIAL GIS 2009), November 4–6, Seattle, WA.

Park, Hyoshin, Ali Haghani, and Xin Zhang. 2016. "Interpretation of Bayesian Neural Networks for Predicting the Duration of Detected Incidents." *Journal of Intelligent Transportation Systems* 20 (4): 385–400.

Peeta, Srinivas, Jorge L. Ramos, and Shyam Gedela. 2000. "Providing Real-Time Traffic Advisory and Route Guidance to Manage Borman Incidents On-Line Using the Hoosier Helper Program."

Ribeiro, Marco Tulio, Sameer Singh, and Carlos Guestrin. 2016. "Why Should I Trust You?: Explaining the Predictions of Any Classifier." In *Proceedings of the 22nd ACM SIGKDD international conference on knowledge discovery and data mining*, 1135–1144. ACM.

Rossi, Thomas, and Chandra R. Bhat, et al. 2014. *Guide for Travel Model Transfer*. Technical Report. United States. Federal Highway Administration.

Saxena, Akrati, Vaibhav Malik, and S. R. S. Iyengar. 2016. "Estimating the Degree Centrality Ranking." In *2016 8th International Conference on Communication Systems and Networks (COMSNETS)*, 1–2. IEEE.

Shunping, Jia, Peng Hongqin, and Liu Shuang. 2011. "Urban Traffic State Estimation Considering Resident Travel Characteristics and Road Network Capacity." *Journal of Transportation Systems Engineering and Information Technology* 11 (5): 81–85.

Wirasinghe, S. Chandana. 1978. "Determination of Traffic Delays From Shock-wave Analysis." *Transportation Research* 12 (5): 343–348.

Wong, Wai, and Sze Chun Wong. 2016. "Evaluation of the Impact of Traffic Incidents Using GPS Data." In *Proceedings of the Institution of Civil Engineers-Transport*, Vol. 169, 148–162. Thomas Telford Ltd.

Wright, Chris, and Penina Roberg. 1998. "The Conceptual Structure of Traffic Jams." *Transport Policy*5 (1): 23–35.

Zaki, Mohammed J., Wagner Meira Jr., and Wagner Meira. 2014. *Data Mining and Analysis: Fundamental Concepts and Algorithms*. New York: Cambridge University Press.

Zhang, Junlong, and Yu Luo. 2017. "Degree Centrality, Betweenness Centrality, and Closeness Centrality in Social Network." In *2017 2nd International Conference on Modelling, Simulation and Applied Mathematics (MSAM2017)*, 300–303. Atlantis Press.